

Experimental Study on Radon motion during Rock Compression

Jiankun Zhao^{1,2}, Liangquan Ge^{1,2,a}, Yaoyao Luo¹ and Yi Gu^{1,2} Qingxian Zhang^{1,2}

¹ Chengdu University of Technology, Chengdu 610059, China

² Key Laboratory of Applied Nuclear Techniques in Geosciences, Chengdu 610059, China

Abstract: A mathematical model to describe the radon motion outside the surface of rocks during the sustained stress on the rocks has been established and an experimental device for monitoring changes of radon concentration has been designed. The theoretic and experimental results show that there is a negative correlation between radon concentration emitted from granite and sandstone rock specimens and the axial pressure loaded on the rock specimens. The maximum error of the radon concentration between theoretic and experimental results is about 10.74%.

Keywords: radon motion, rock compression, mathematical model, experiments

1 Introduction

As an effective natural tracer, radon has been widely used in many applied physics fields such as exploration, engineering investigation and other applied geophysics. It is also considered a sensitive physical method to predict the earthquake and has been ordinarily monitored in a number of Earthquake Monitoring Stations[1-3]. There are many experts that, at home and abroad have investigated the relevance between the earthquake and the anomalies of radon concentration in rocks for a long time. As early as 1944, on the eve of the 8.3 magnitude earthquake taking place in southwest of Japan, the mutation of Radon concentration has aroused the great attention of Hatuda[4]. In 1991, Houlub put forward his research result about the condition of radon exhalation under uniaxial pressure [5]. The physical mechanism of radon motion is qualitatively explained that the tectonic stress impacts on the primary fracture of geologic body, which influences the migration channels of radon[6-8]. This paper attempts to provide a mathematical model to describe the radon motion outside the surface of rocks and designs an experimental device to prove it.

2 The Relationship between Stress and Radon Concentration on the Surface of Rocks

During the diagenesis process, there are a large number of finer textures, such as fractures and pores, existing insiderocks upon the effects of natural conditions including cooling, dilation and stress. These finer textures are regarded as the natural systems and storage spaces for free radon. If the macroscopic stress effected on the rock continually, the finer textures will change with it. A power function can be utilized to express the relationship between porosity and pressure [9,10]:

$$P = P_0 - A\sigma^n \quad (1)$$

Where, P and P_0 is the porosity of rocks at the stress pressure with σ and at normal pressures (%), respectively; A and n are both constants ($n=0.73$); σ is effective stress (MPa/cm²).

The radon concentration on the surface of rocks can be defined as:

$$N_K = kN_P \quad (2)$$

Where, N_K is the radon concentration on the surface of

^a Corresponding author: glq@cdut.edu.cn

rocks (Ci/cm^3); N_p is the radon concentration in fractures of rocks (Ci/cm^3); k is called the escaping coefficient of radon from a rock which is defined as the ratio of the radon concentration on the surface of a rock to the radon concentration in fractures of the rock.

If the decay of radium and radon is in radioactivity decay equilibrium in which the decay rate of radium is equal to that of radon in rocks, the radon concentration in fractures of rock can be given by [2]

$$N_p = P\rho g\eta \quad (3)$$

Where, ρ is the density of the rock (g/cm^3); g is the specific activity of the natural ^{226}Ra in the rock (g/g); η is the emanation coefficient of radon of the rock, which is defined as the ratio of the radon concentration in fractures of a rock (N_p) to the total radon concentration of the rock.

Eq. (2) and Eq. (3), we have:

$$N_K = kP\rho g\eta \quad (4)$$

We denote an effective escaping coefficient K which is equals to $k\eta$. From Eq. (1) and Eq. (4), we have:

$$N_K = K\rho g(P_0 - A\sigma^n) \quad (5)$$

Based on above equations, the radon concentration on the surface of rocks is not only direct proportional to the specific activity of ^{226}Ra in the rock, but also to the effective stress (σ) loaded on the rock. When the compressive stress loaded on a rock increases, the radon concentration on the rock will decreases in the way of n power function of σ .

Through the way of the free diffusion, the radon in air migrates along the distance that can be described as:

$$N_x = N_K e^{-\sqrt{\frac{\lambda}{D}} \cdot x} \quad (6)$$

Where, x is the migration distance in air (cm); λ is the decay constant of ^{222}Rn ($2.1 \times 10^{-6} \cdot \text{s}^{-1}$); D is the

diffusion coefficient at the normal temperature and pressure (cm^2/s).

$$N_x = K\rho g(P_0 - A\sigma^n) e^{-\sqrt{\frac{\lambda}{D}} \cdot x} \quad (7)$$

Taking differential form of Eq. (7), then we get the Eq. (8):

$$\frac{dN_x}{d\sigma} = -K\rho g n A e^{-\sqrt{\frac{\lambda}{D}} \cdot x} \sigma^{n-1} \quad (8)$$

Where, the ratio of dN_x to $d\sigma$ is defined as the sensitivity of the radon concentration effected by stress ($\text{Ci}/\text{cm}^3\text{Pa}$); minus indicates the negative correlation; if the density and specific activity of rocks are given, the sensitivity is only related to the stress loaded on the rock.

3 Experiment and Measurement of Radon

3.1 Specimen Preparation and Experimental Facility

Both granite and red sandstone rocks are specimen for the experiments of radon. The main mineral compositions of granite, specimen from Longmen Mountains Fault Zone where Wenchuan Ms 8.0 earthquake took place in 2008, are mica, quartz, feldspars and pyroxene; the red sandstone is composed of calcium-iron cementation and the grain sizes of minerals is from 0.25mm to 0.5mm. The main physical parameters of granite and red sandstone are listed in **Table 1**. The specific activity of the granite and red sandstone are determined by the Key Laboratory of Applied Nuclear Techniques in Geosciences, Sichuan, China. The design and cutting size of experimental specimens refer to the national standard 'The standard of the engineering rock mass test method' (GBT50266- 1999), and then specimens do the drying treatment for 24h.

Table 1 The main physical parameters of granite and sandstone specimens

specimens	Size/cm	Specific activity of Ra-226/Bq/kg	Specific activity of Th-232 Bq/kg	Compressive strength/ MPa
Granite	$\phi 5 \times 10$	10.27	13.31	100
Sandstone	$\phi 5 \times 10$	18.74	33.55	19

The Uniaxial stress experiment is accomplished in the State Key Laboratory of Geohazard Prevention and Geoenvironment Protection with triaxial creep testing machine. The pressure loaded on the rock specimen strictly maintains during the experiment. For the purpose, a double-deck sealing device without air convection was designed as shown in Fig. 1. The device is made up with the rock specimen, radon accumulating detectors and sealing cover which consists of an oblong-shaped rack and double thin plastic coating. The rock specimen is located in center and three radon detectors are parallel to each other 10cm away from the specimen. Meanwhile, three detectors are placed into another device without specimens to measure the background count [11].

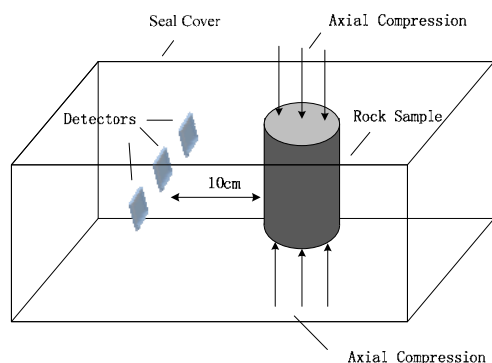


Fig.1 Schematic sketch of Radon measurement device

At first, a test of breaking, in which the pressure loaded on specimens is high enough to break the rock, has been done to determine the maximum uniaxial pressure. The results show that the maximum uniaxial pressures of granite and sandstone are about 100MPa and 19MPa, respectively. So, the proper gradient is set as: 30MPa、60MPa、90MPa for granite and 5MPa、10MPa、15MPa for red sandstone. Under the given uniaxial stress, the radon is accumulated for 10 days. According to the law of radon decay and accumulation, 10 days is about three times of half-life for ^{222}Rn and the accumulating amount of ^{222}Rn in 10 days is about 84% of total accumulation amount.

3.2 Detection and Calibration

CR-39 solid-state track detector is chosen as the radon accumulation detector. When a alpha particle emitted from radon and its daughters strike the CR-39

detector, a damaged latent track may be formed along alpha passed path. The latent track can expand to be observed and counted with optical microscope by means of chemical etching method. The solution composition of Chemical etching is: the amount-of-substance concentration of KOH solution of 6.5mol/L and 300 ml is need for every 10 detectors. Keep the detectors in the etching solution 10 hours at 70 degrees Celsius by water-bath heating. Then count the amount of the latent tracks on the materials through the ‘α Image Acquisition System’ developed by CDUT.

The relationship between track population on the detector and radon concentration can be expressed as:

$$N_x = \frac{L}{T \cdot F_R \cdot S} \quad (9)$$

Where, N_x is the air radon concentration on the point where the radon detector located (Bq/m^3); L is the number of the tracks; F_R is the radiation coefficient ($\text{cm}^2/\text{Bq} \cdot \text{h}/\text{m}^3$); T is the irradiation time (h); S is the effective-area of the detector (cm^2). As the irradiation time is given, the radon concentration is proportional to the track population. Thus, Eq. (9) becomes:

$$N_x = aI \quad (10)$$

Where, $a=1/(T \cdot F_R)$ is defined as the calibration factor; $I=L/S$ is the track population. The calibration for CR-39 solid-state nuclear track detector is accomplished in the Radon Chamber in CDUT. The calibration factor is 0.0356 Bq/m^3 and the reproducibility is 2.9%.

4 Results and Discussion

Radon concentrations in the closed device under the different pressure are listed in **Table 2**. The first column in **Table 2** is the axial pressure loaded on the rock specimens for 10 days. The means of concentration on three detectors are listed in the second column. The radon concentrations, according to Eq. (9), are shown in the second column. **Fig. 2** represents the radon concentrations for granite and red sandstone. The results at 100MPa pressure for granite and at 19MPa pressure for red sandstone are obtained under the conditions of broken rock specimens.

The concentration decrease as the uniaxial stress increases. The concentration just $9.6 \text{ Bq} \cdot \text{m}^{-3}$ at 90MPa pressure loaded on granite specimens that is only 32% of the natural specimen at ambient pressure conditions. Obviously, it can be explained as radon is much more difficult to migrate outside from the pores and fractures of granite specimens that is narrowed or closed when uniaxial stress is loaded on the granite specimens.

The uniaxial stress experiments show a complex result (**Fig. 2** and **Table 2**). Firstly, when 5MPa pressure is loaded on red sandstone specimens, the radon concentration from the red sandstone is higher than that of the natural sample at ambient pressure conditions. It is because that sandstone consists of hard mineral grain and weak cement, so, it is easy to expand the pores and fractures when primary pressure loaded. Secondly, with the uniaxial stress increasing the concentration are decreasing. The concentration at 15MPa are just 60% of those at 5MPa.

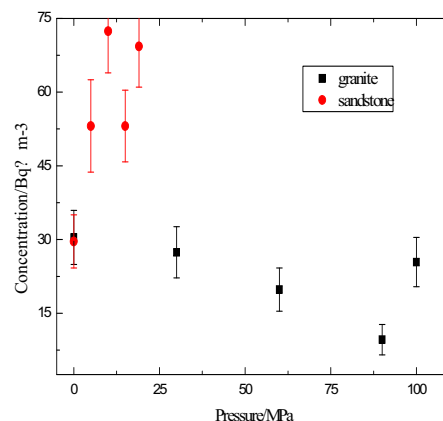


Fig.2 relationship between number of tracks and axial pressure

Table 2 Data showing the relationship between radon concentration and axial pressure

	Pressure /MPa	Concentration /Bq · m ⁻³
granite	0	30.4±5.5
	30	27.4±5.2
	60	19.8±4.4
	90	9.6±3.1
	100	25.4±5.0
sandstone	0	29.6±5.4
	5	88.6±9.4
	10	72.4±8.5
	15	53.1±7.3
	19	69.3±8.3

When the rock specimens are broken, such as, at 100MPa and at 19MPa in **Fig. 2**, the concentration of the radon increase. That is to say, the Eq. (3) will be no long applicable. Evidence to date indicates that there is a positive correlation between rupture degree and radon exhalation rate [12].

Table 3 is the normalized results of theoretical calculation and experiment. The theoretical data of radon concentration is based on Eq. (7). **Fig.3** is the normalized theoretical curves and the experimental scatter diagrams of the relationship between the radon concentration from

rock specimens and uniaxial stress loaded on rock specimens. It shows a good agreement between theoretical and experimental results. The relative errors between them are 10.74% and -8.68% under the condition of 60MPa and 90MPa for granite while 6.7% and 10.37% under the condition of 10MPa and 15MPa for red sandstone. From **Fig.3** and **Table 3**, we also see that the concentration of the radon emanated from red sandstone is more sensitive to uniaxial stress than that from granite to the changes of axial pressure. Also, the radon concentration from red sandstone is 3 to 5 times than that from granite.

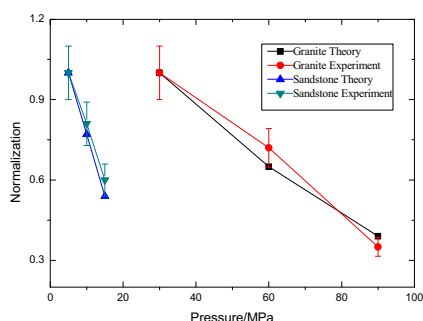


Fig.3 The relationship between radon concentration and axial pressure after normalization

Table 3 The contrast analysis of theoretical calculation and experimental results

Pressure /MPa	Normalization		Relative error/%
	Theory	Experiment	
30	1.00	1.00	/
60	0.65	0.72	10.74
90	0.39	0.35	- 8.68
5	1.00	1.00	/
10	0.77	0.81	6.70
15	0.54	0.60	10.37

5. Conclusions

Both the theoretic and experimental results indicate that there is a negative correlation between the concentration of radon emitted from rock and the uniaxial pressure loaded on the rock. The relative error of radon concentrations obtained from theoretic calculation and

experimental results is less than 10.74%.

Acknowledgements

The authors gratefully acknowledge the financial support of: (1) National Natural Science Foundation of China through Grant No. 41074093 entitled ‘‘Research on mechanism of earthquake radon anomaly’’, (2) The National High - tech Research and Development Program of China through Grant 2012AA061803 entitled ‘‘Development of high precision nuclear radiation spectrometry’’.

References

1. Y Zhang, R Z Hua, B S Shi. *Radioactive Prospecting Methods* (BJ Atom Ener Pres, 1985)
2. Chengdu Geological Institute. *Radioactive Exploration Methods*. (BJ Atom Ener Pres, 1978)
3. Y Gu, L Q Ge, G X Wang, et al. *Jour of Engi Geol. J.* **17**, 296(2009)
4. A H Sultanhuojiaye. *The application of radioactive gas in the study of geological process* (BJ Seis Pres, 1981)
5. M Singh, R C Ramola, B R Singh, et al. *Nucl Trac and Radi Meas. J.* **19**,417(1991)
6. X H Han, G X Wang. *Jour of Taiyuan Univ of Tech.* **31**, 101 (2000)
7. L Chen, J L Xie, L Huang. *Rad Pro Bul. J.* **18**, 28(1998),
8. J Yan, L Q Ge, G J Zou, et al. *Nucl Tech. J.* **36**, 27 (2013)
9. J Geertsma. *AIME. R.* 331 (1957)
10. K W Vander. *AIME. R.* 179 (1959)
11. J K Zhao, L Q Ge, G J Zou, et al. *Nucl Tech. J.* **36**, 110404 (2012)
12. G W Luo, X Z Shi. *Acta Seis Sini. J.* **2**, 198(1980)